Chapter 7
System Identification of an MDOF Experimental Structure with a View Towards Validation and Verification

K. Worden, O.D. Tiboaca, I. Antoniadou, and R.J. Barthorpe

Abstract Validation approaches can determine the degree of accuracy of simulated models representing real structures. Therefore these approaches should deal with concepts concerning fidelity-to-data, the uncertainty quantification and the comparative metrics i.e. measures that quantify the level of agreement between simulation and experimental outcomes. In the context of nonlinear systems associated with nonlinear models additional care should be taken when attempting to perform a validation scheme, in order to evaluate the examined models, due to bifurcations that may occur.

In this paper, experimental datasets from a laboratory based three-story building structure are used in order to calibrate the parameters of a physics-based model using system identification methods. The structure described here is linear; however, the work is a necessary precursor to the investigation of the behaviour of the structure when nonlinearity is introduced in the form a cantilever beam impacting the highest story of the building for a specific range of excitations. In this study the linear model is identified using experimental data and the sensitivity of model predictions is examined when the parameters of the model are varied.

Keyword System identification

7.1 Introduction

This study focuses on the application of methods of Verification and Validation (V&V) to nonlinear structural dynamics models. V&V of numerical models is a pressing issue across science and engineering and one that is attracting increasing interest from both the industrial and academic research communities. Reliance upon the predictions of complex simulations has advanced to the point of dominating the test and analysis process in many applications. This is particularly the case in applications where experimental testing is either prohibitively expensive or simply not feasible, the study of structural response to extreme events being one such example. The aim of model validation is to provide a principled means of assessing the credibility that may be ascribed to numerical model predictions. In recent years a number of application-specific guidelines have been proposed for implementing this process. Among the first such frameworks to focus on physics-based engineering models was that produced in 1999 by the AIAA for computational fluid dynamics (CFD) problems [1]. These have been followed more recently by as series of standards introduced by the American Society of Mechanical Engineers (ASME), currently comprising the ASME Guide for V&V in Computational Solid Mechanics in 2006 [2] and the Standard for Verification and Validation in Computational Fluid Dynamics and Heat Transfer in 2009 [3]. These texts provide a solid foundation for the study of validation methods and many of the more general aspects of these frameworks are transferable to problems in structural dynamics. However, validation of nonlinear dynamical models presents additional challenges that are yet to be fully addressed in the research literature. An issue of particular interest is how to account for potential bifurcations in the frequency response of a non-linear system.

This paper presents some of the precursor analyses required as part of a broader framework for V&V of nonlinear systems. The layout of the paper is as follows. The experimental rig adopted for the study is introduced in Sect. 7.2. Sections 7.3 and 7.4 introduce tools for system identification and analysis and present results of their application to the bookshelf structure. Discussions of results and directions for future work are given in Sect. 7.5.

K. Worden (✉) • O.D. Tiboaca • I. Antoniadou • R.J. Barthorpe
Dynamics Research Group, Department of Mechanical Engineering, University of Sheffield, Mappin Street, Sheffield S1 3JD, UK
e-mail: k.worden@sheffield.ac.uk

M. Mains (ed.), *Topics in Modal Analysis, Volume 10*, Conference Proceedings of the Society for Experimental Mechanics Series, DOI 10.1007/978-3-319-15251-6_7

7.2 The Experimental Rig and Data Capture

For the purposes of the present work, a small-scale simulated shear building model was constructed. This was chosen to correspond closely with a structure previously designed and built at Los Alamos National Laboratories (LANL). Within LANL, the experimental rig was referred to informally as the 'bookshelf' rig and this informal nomenclature is also adopted here. The bookshelf structure, illustrated in Fig. 7.1 has four levels, floors or shelves, with the lower level being considered the base. Each shelf/floor is composed of a substantial rectilinear aluminium block with a mass of 5.2 kg and dimensions $35 \times 25.5x \times 0.5$ cm ($L \times w \times h$). The shelves are joined by upright beams at each corner; each beam having a mass of 238 g and dimensions $55.5 \times 2.5 \times 0.6$ cm. The blocks used to connect the main plates and the upright beams have a mass of 18 g and dimensions $2.5 \times 2.5 \times 1.3$ cm. For each block, four bolts were used, each of Viraj A2-70 grade and with a mass of 10 g. The structure was mounted on a rail system which was securely clamped onto a substantial testing table. In order to introduce the excitation into the structure, an electrodynamic shaker with a force transducer was connected to the base. The output response of the structure was recorded using four accelerometers positioned, as shown in the pictures, at the middle of each main plate.

So far, the system is linear, and the intention of the first identification tests was that it remain so in order to simplify the identification problem. However, as the longer term goal of this work was to consider nonlinear systems, provision was made for nonlinearity. In the original LANL structure, nonlinearity was introduced via a comparatively complex series of bumpers connected between shelves; in the current structure, nonlinearity is introduced in a much more basic fashion in order to impose simpler equations of motion. The nonlinearity here will be introduced via a vertical cantilever beam which contacts (via a bolt) the topmost shelf of the structure at negative displacements of that shelf.

The experimental data were acquired using an LMS CADA system connected to a SCADAS-3 interface. A total of 93,184 points per channel were recorded at a sampling frequency of 1024 Hz. Lateral accelerations were recorded for each shelf from piezoelectric accelerometers fixed to the edges. 'FRFs' (transmissibilities) between the relative accelerations of the floor and the base acceleration are given in Fig. 7.2; the structures shown indicate that a three-DOF model of the rig is likely to capture the main dynamics.

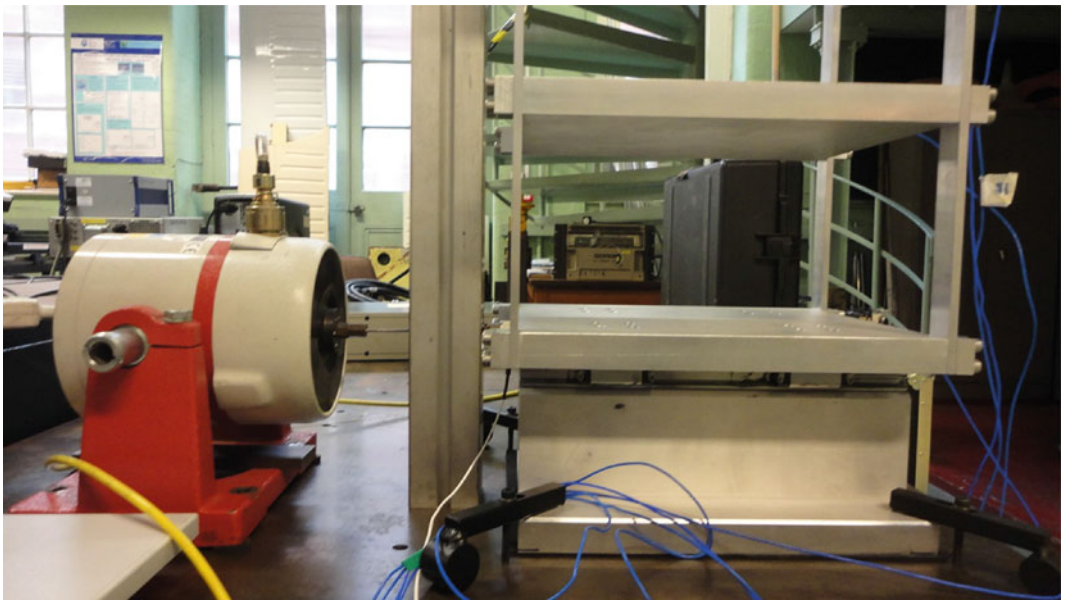

Fig. 7.1 The 'bookshelf' experimental rig showing shaker attachment and guide rail system

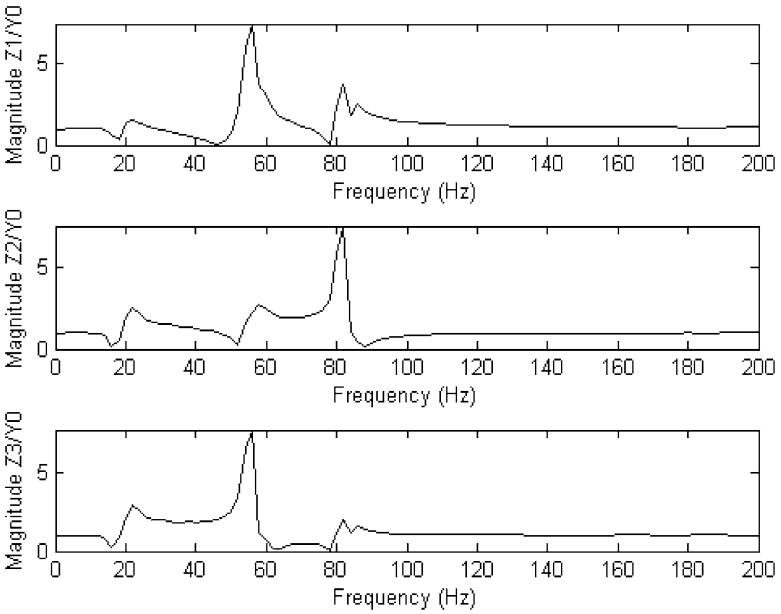

Fig. 7.2 'FRFs' between the base acceleration of the rig and the relative accelerations of the upper floors

7.3 System Identification Using Self-Adaptive Differential Evolution (SADE)

For the sake of completeness, a brief overview of the basic Differential Evolution (DE) and SADE algorithms will be given here; for more detail, the reader is referred to the original papers [11, 12]. As in all evolutionary optimisation procedures, a population of possible solutions (here, the vector of parameter estimates), is iterated in such a way that succeeding generations of the population contain better solutions to the problem in accordance with the Darwinian principle of survival of the fittest. The problem is framed here as a minimisation problem with the cost function defined as a normalised mean-square error between the measured data and that predicted using a given parameter estimate. Having established by FRF analysis that the base-excited system appears to correspond well to a three-DOF system, the model equations considered were,

$$\begin{aligned} m_1\ddot{z}_1 + c_1\dot{z}_1 + c_2(\dot{z}_1 - \dot{z}_2) + k_1 z_1 + k_2(z_1 - z_2) &= -m_*\ddot{y}_0 \\ m_2\ddot{z}_2 + c_2(\dot{z}_2 - \dot{z}_1) + c_3(\dot{z}_2 - \dot{z}_3) + k_2(z_2 - z_1) + k_3(z_2 - z_3) &= -m_*\ddot{y}_0 \\ m_3\ddot{z}_3 + c_3(\dot{z}_3 - \dot{z}_3) + k_3(z_3 - z_2) &= -m_*\ddot{y}_0 \end{aligned} \tag{7.1}$$

where the $\{z_i = y_i - y_0 \ : \ i = 1, \ldots, 3\}$ are displacement coordinates relative to the base displacement. As discussed above, the rig was operated in its linear condition in order to acquire data for the identification. As it is not clear what the actual masses are prior to the identification, an estimate m_* is used for the RHS of the equations. The estimate is based on the physical masses of the shelves and associated fixings, Including m_1, m_2 and m_3 in the parameter vector $\underline{\theta} = (m_1, m_2, m_3, c_1, c_2, c_3, k_1, k_2, k_3)$ allows the identification algorithm to correct for the contribution of the vertical beams etc. Based on the design geometry and materials, m_* was taken here as 5.475 kg.

The cost function referred to above was defined here in terms of the prediction errors associated with each DOF. A set of Normalised Mean-Square-Errors (NMSEs) J_i were defined by,

$$J_i(\underline{\theta}) = \frac{100}{N\sigma^2_{\ddot{z}_i}} \sum_{i=1}^{N} (\ddot{z}_i - \hat{\ddot{z}}_i(\underline{\theta}))^2 \tag{7.2}$$

where $\sigma^2_{\ddot{z}_i}$ is the variance of the measured sequence of relative accelerations and the caret denotes a predicted quantity; N is the number of 'training' points used for identification. The total cost function J was then taken as the average of the J_i. Previous experience has shown that a cost value of less than 5.0 represents a good set of model predictions (or parameter estimates).

In order to generate the predictions $\hat{\ddot{z}}_i$, the coupled Eqs. (7.1) were integrated forward in time in Matlab [8] using a fixed-step fourth-order Runge–Kutta scheme for initial value problems [10]. A better solution could potentially be found by using

an adaptive solver like the $(4, 5)$th-order Runge–Kutta method for the solution of non-stiff problems encapsulated in the Matlab function ode45; however, it was shown in [16] that the use of the adaptive scheme in the context of evolutionary system identification can lead to strange results. The excitations for the predictions were established by the measured base accelerations $\ddot{y}_0$ and the initial estimate m_*. Although a great deal of data were measured in the experiments, the SADE identification scheme is computationally expensive, with the main overhead associated with integrating trial equations forward in time. For this reason, the training set or identification set used here was composed of only $N = 700$ points. To avoid problems associated with transients, the cost function was only evaluated from the final 500 points of each predicted record.

Once the data were generated, the SADE algorithm was applied to the identification problem using a parameter vector $\underline{\theta}$. The standard DE algorithm of reference [11] attempts to transform a randomly generated initial population of parameter vectors into an optimal solution through repeated cycles of evolutionary operations, in this case: mutation, crossover and selection. In order to assess the suitability of a certain solution, the cost function referred to above was used; this casts the identification in the form of a minimisation problem.

Figure 7.3 shows a schematic for the procedure for evolving between populations. The following process is repeated with each vector within the current population being taken as a *target vector*; each of these vectors has an associated cost J defined above. Each target vector is pitted against a *trial vector* in a selection process which results in the vector with lowest cost advancing to the next generation. The process for constructing the trial vector involves variants of the standard evolutionary operators: mutation and crossover.

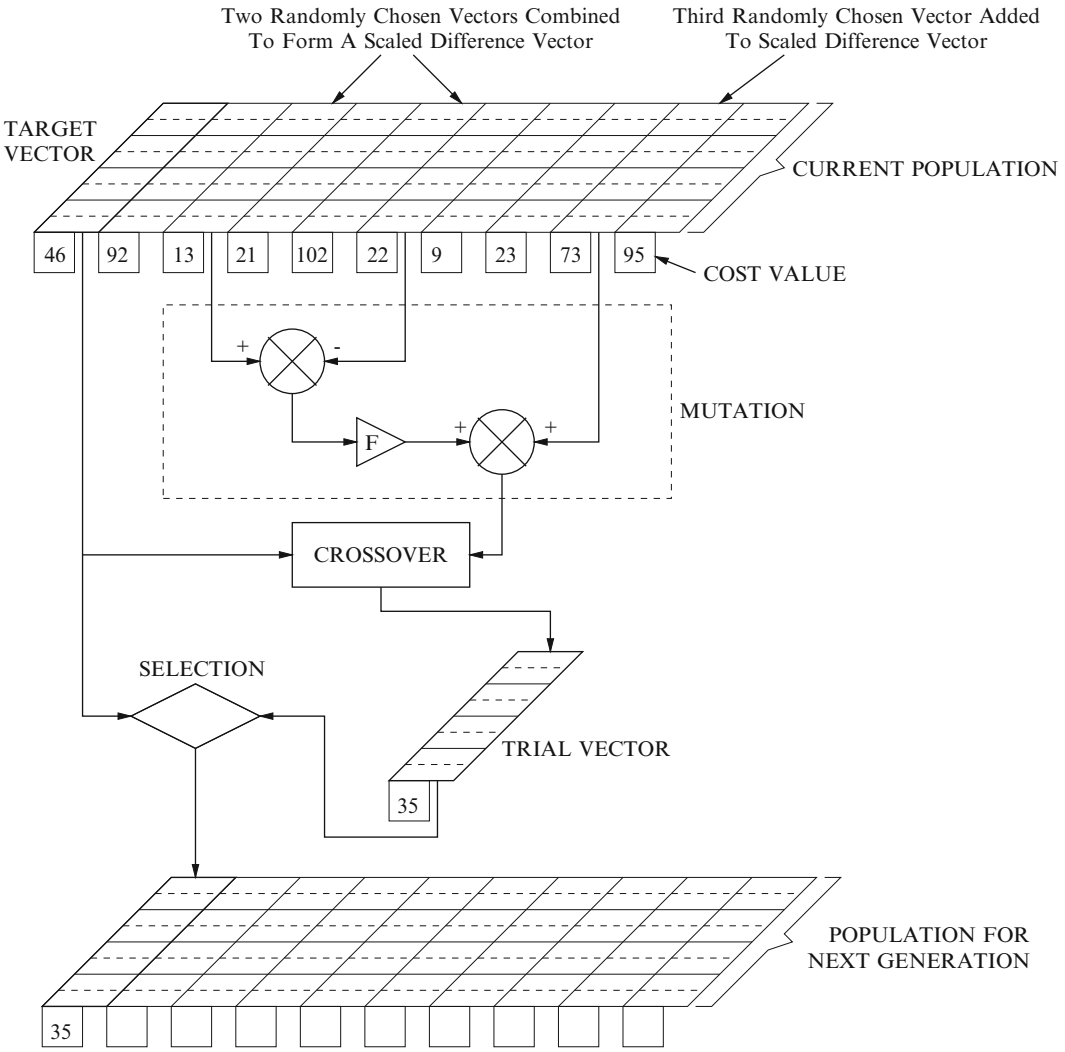

Fig. 7.3 Schematic for the standard differential evolution algorithm

The mutation procedure used in basic DE employs vector differentials. Two vectors A and B are randomly chosen from the current population to form a vector differential $A - B$. A *mutated vector* is then obtained by adding this differential, multiplied by a scaling factor, F, to a further randomly chosen vector C to give the overall expression for the mutated vector: $C + F(A - B)$. F is often found have an optimal value between 0.4 and 1.0.

The *trial vector* is the child of two vectors: the target vector and the mutated vector, and is obtained via a crossover process; in this work uniform crossover is used. Uniform crossover decides which of the two parent vectors contributes to each chromosome of the trial vector by a series of $D - 1$ binomial experiments, where D is the dimension of the problem i.e. the number of parameters in the model. Each experiment is mediated by a crossover probability C_p (where $0 \leq C_p \leq 1$). If a random number generated from the uniform distribution on [0,1] is greater than C_p, the trial vector takes its parameter from the target vector, otherwise the parameter comes from the mutated vector.

This process of evolving through the generations is repeated until the population becomes dominated by only a few low cost solutions, any of which would be suitable. The core of the SADE algorithm is essentially that of DE, the only real difference being that, in SADE, F and C_p are adapted generation by generation in order to arrive at optimal values. Furthermore, SADE can select between different mutation strategies in addition to the basic DE strategy described above in order to optimise its performance; the specific additional strategies applied here are the same as those described in [15].

In this case, the SADE algorithm was initialised with a population of randomly selected parameter vectors or individuals. The parameters were generated using uniform distributions on specified initial ranges. As in all iterative optimisation schemes, the initial estimates can prove critical; here, estimates based on engineering judgement were used. The masses in the model were not considered as a problem, as the inertia of the system was considered very likely to be dominated by the shelves and fixings, it was expected that the true values would be close to the estimate m_* given above. For this reason, a short range $[4.5, 6.0]$ was taken for the initial population. The situation with the stiffness parameters is a little more complicated as it is not clear what the appropriate boundary conditions are the upright beams connecting the floors. An approximate value of $k_* = 5.2 \times 10^5\,\mathrm{N/m}$ can be obtained by assuming encastre conditions; however, the true value may vary substantially from k_* if the bolts do not impose a true fixed condition, for example. Because of the uncertainty in the initial physical estimates of the stiffness, the initial ranges for SADE were taken on roughly an order of magnitude below and above k_* i.e. $[5 \times 10^4, 5 \times 10^6]$. Taking into account the values of m_* and k_* and assuming damping ratios in the vicinity of 0.1 % for aluminium, the initial ranges for the damping parameters were estimated at $[0.1, 10.0]$, again an order or magnitude below and above a nominal value of $c_* = 1.0\,\mathrm{N\,s/m}$.

A population of 100 individuals was chosen for the SADE runs with a maximum number of generations of 200. In order to sample different random initial conditions for the DE algorithm, ten independent runs were made. The other parameters chosen used for SADE were a starting value for F of 0.9 and a starting value for C_p of 0.5 (these values proved to be effective in a number of previous studies; this completes the specification of SADE for the problem of this paper.

Each of the ten runs of the DE algorithm converged to a good solution to the problem in the sense that cost function values of around 2 % or below were obtained in all cases; the summary results are given in Table 7.1. The best solution gave a cost function value of 1.591. A visual comparison of the 'true' experimental responses and predicted responses for the best parameter set is given in Fig. 7.4. This comparison is based upon a set of testing data that was distinct from the training data used to fit the parameters.

The results are interesting. Although there are only small variations in the prediction errors, the coefficients of variation (standard deviation of estimate/mean of estimate) are quite high for a number of the parameters. This indicates that the errors are rather insensitive to the parameters. One of the questions usually investigated in the validation of models is this

Table 7.1 Parameter estimates from ten independent SADE runs

Parameter	Best	Maximum	Minimum	Mean	Standard deviation	Coefficient of variation
m_1	5.144	5.228	5.023	5.109	0.054	0.011
m_2	5.587	5.813	5.558	5.656	0.076	0.013
m_3	5.264	5.456	5.264	5, 348	0.068	0.013
c_1	6.681	10.00	4.725	5.918	3.290	0.556
c_2	0.476	0.973	0.100	0.312	0.304	0.975
c_3	3.411	4.045	0.100	1.423	1.493	1.049
k_1 ($\times 10^{-5}$)	1.156	1.219	0.500	0.856	0.333	0.390
k_2 ($\times 10^{-5}$)	5.874	6.920	5.333	6.113	0.429	0.070
k_3 ($\times 10^{-5}$)	3.126	4.374	0.500	2.661	1.095	0.411
J	1.591	2.021	1.591	1.773	0.156	0.088

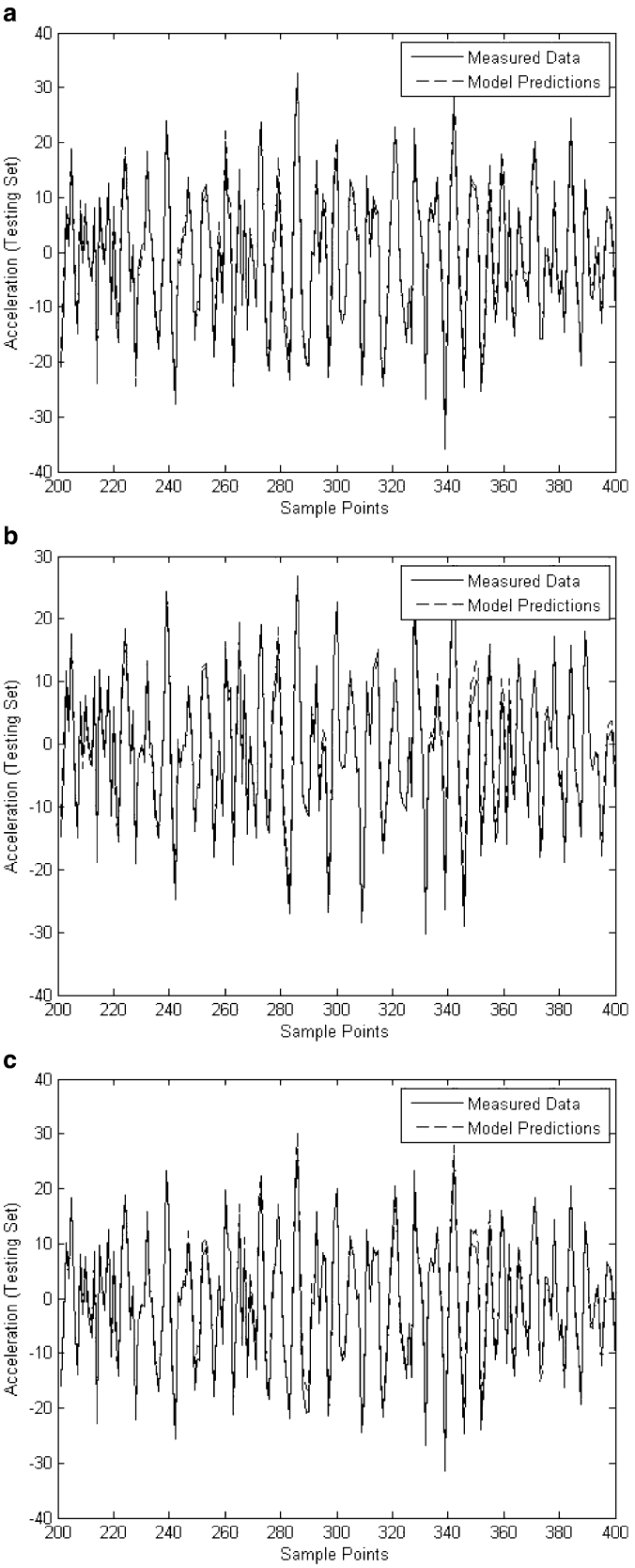

Fig. 7.4 SADE model predictions on testing data: (**a**) $\ddot{z}_1$, (**b**) $\ddot{z}_2$, (**c**) $\ddot{z}_3$

question of sensitivity; how is the uncertainty in an outcome (prediction error) related to the uncertainty in the inputs (model parameter estimates). This is considered in more detail in the following section, where a Bayesian sensitivity analysis is applied. The insensitivity of the errors in this case is most likely related to the fact that only a small training set is used; this would normally be a simple matter to deal with at the expense of a little more computational effort; however, this is not addressed here as the objective of the paper is to look at issues associated with sensitivity and fidelity and the current situation allows interesting discussion.

7.4 Bayesian Sensitivity Analysis

The Sensitivity Analysis (SA) technique used here is based on a non-parametric probabilistic approach as detailed in [9]. Each uncertain input parameter is represented as a probability distribution, and a Gaussian process emulator (fast running model or surrogate model) is fitted using multiple runs of the model as dictated by a Design-of-Experiments (DOE). From this emulator, statistical quantities relating to sensitivity and uncertainty can be inferred directly; for example, output uncertainty distributions and main effects. Importantly, this requires no additional runs of the original model for each sensitivity measure, unlike conventional SA methods detailed for example in [14]. Furthermore, the advantage of using Gaussian process regression is that the uncertainty of the emulator fit is itself quantified, giving the analyst a very pragmatic quantification of the uncertainty in the data. A very brief summary of the main points of the algorithm will be given, the reader is referred to the original papers for more details.

7.4.1 Gaussian Process Regression

Any computer model can be regarded as a function of its inputs: $f(\underline{x})$. Although this function is deterministic and governed by known mathematical relationships, it is often of such complexity as to be considered mathematically intractable. From a practical point of view, $f(\underline{x})$ could be regarded as an unknown function, given that one does not know the output for a given set of inputs until one has actually run the model. If, however, one samples the function (model) at a number of carefully chosen input points, it is possible to fit a response surface that can predict the output of the model for any point in input space without having to run the simulation itself. Although the idea of modelling a model (metamodelling) may seem a little abstract, for simulations that are computationally expensive it is a useful tool, since any approach for uncertainty analysis requires multiple runs of the model under investigation.

A particular approach to formulating the metamodel or emulator that has gathered interest in recent years is the use of Gaussian process regression [6, 7, 15]. Gaussian processes are an extension of a multivariate Gaussian probability distribution. Whereas most forms of regression return a crisp value $f(\underline{x})$ for any given $\underline{x}$, a Gaussian process returns a Gaussian probability distribution. Thus for a function, the Gaussian process can be considered as a multivariate Gaussian distribution, where the dimension of the multivariate distribution can be thought of as the resolution of the function, or the number of predictive points. In the case detailed here, the resolution need not be specified, since one is not interested in predicting particular output points, but rather quantities pertaining to the whole range of output space.

Gaussian processes adhere to the Bayesian paradigm, that is, a number of prior assumptions are made about the function being modelled, and then training data (samples from the model) are used to update and evaluate a posterior distribution over functions. A key assumption is that the model is a *smooth* function of its inputs; it is this that allows extra information concerning the response to be gained at reduced computational cost. No mathematical details will be given here: the reader is referred to [6, 7, 13]. The important point for the current context is that a model is formed which can estimate accurately what the cost function J is corresponding to a given set of parameter estimates $\underline{\theta}$ *without* integrating the equations of motion forward in time.

The dependence of the emulator on training data means that some model runs are always required. The advantage of the Bayesian sensitivity approach is that, typically far fewer runs are needed to train the emulator than would be needed for a full Monte Carlo sensitivity analysis. To deal with the sampling of training data in as principled manner as possible, ideas of experimental design are applied and a maximin Latin hypercube design (maximin LHD) generated using the GEM-SA software [5] is used here.

7.4.2 Inference for Sensitivity Analysis

Several quantities can be inferred from the GP regression model described above, that are relevant to sensitivity analysis. Fundamental quantities such as the mean and variance of the output distribution can be evaluated, as well as main effects, interactions and sensitivity measures for input parameters based on their contribution to output variance [ref].

The results presented here will be for variance and sensitivity indices. Variance-based methods are widely used in sensitivity analysis. This involves quantifying the proportion of output variance for which individual input parameters are responsible. In particular, sensitivity can be measured by conditional variance,

$$V_i = \mathrm{Var}\{E(J|\theta_i)\} \tag{7.3}$$

which is the expected value of the contribution of the input variable θ_i to the output variance i.e. the uncertainty in J. (Note that this is also commonly known as the main effect index (MEI)). This can be extended to measure conditional variance of interactions of inputs, i.e. the output variance resulting from co-varying of two parameters θ_i and θ_j, and so on for higher order interactions. Although this approach allows detailed insight into the effects of combinations of inputs on output uncertainty, it can be time-consuming to examine all possible interaction permutations for models with many input dimensions. An alternative sensitivity measure [4], describes the output variance that would remain if one were to learn the true values of all inputs except θ_i,

$$V_{Ti} = \mathrm{Var}(J) - \mathrm{Var}\{E(J|\underline{\theta}_{-i})\} \tag{7.4}$$

where the notation $\underline{\theta}_{-i}$ means the vector of all parameters *except* θ_i. This measure, called the total sensitivity index (TSI), measures the variance caused by an input θ_i and *any* interaction of any order including θ_i. It allows a more holistic view of the uncertainty attributed to each input, but does not give any details as to how it is distributed between main effects and interactions. Between the MEIs and TSIs, a detailed view of the sensitivities of inputs and their interactions can be gained. The advantage of the GP regression emulator is that the functional form of the emulator allows the variance and sensitivity measures to be evaluated as closed form integrals.

7.4.3 Results

As mentioned above the analysis carried out here used the code GEM-SA [5]. In total 200 design points for the Gaussian process emulator were generated as a Latin Hypercube Maximin design. The input parameter distributions were taken as uniform over the ranges assuming for the initial populations used for the SADE analysis. Following the regression stage, the variances and TSIs were computed and the results are given in Table 7.2.

It appears that the main contributors to output variance are stiffnesses, note by far the biggest proportion of output uncertainty comes from interactions; this makes sense because the things that determine the physics of the response i.e. natural frequencies and damping ratios are actually combinations of the basic physical parameters: masses, dampings and stiffnesses.

Table 7.2 Results of Bayesian sensitivity analysis

Parameter	Main effect index	Total sensitivity index
m_1	1.66	14.49
m_2	1.59	25.34
m_3	0.11	0.11
c_1	0.14	0.15
c_2	0.80	20.49
c_3	0.46	6.80
k_1	15.32	52.04
k_2	12.46	58.98
k_3	2.59	35.78
Interactions	69.83	–

7.5 Discussion and Conclusions

The contribution of this study is to demonstrate two of the tools required for model development and validation in structural dynamics. The focus of the SADE system identification exercise detailed in Sect. 7.3 is on improving fidelity-to-data through test-analysis correlation. The method was applied here to the parameters of a linear model using data acquired from the experimental structure, with the results indicating that it is possible to identify a physically feasible set of parameters with a good level of consistency between independent executions of the algorithm. The prediction errors of the resulting model were in this case evaluated using testing data distinct from the training data, although drawn from the same experiment. The derived model was found to perform well in this case although—as expected—the error metric was observed to be higher for the testing data than for the training data. The next step for this work is to evaluate the validity of the derived model form for more challenging scenarios, discussed below.

The second part of the study focused on developing a better understanding the model through application of sensitivity analysis. In this case a global method for sensitivity analysis was adopted based upon Bayesian inference. A particular feature of the structure under study is that a major component of its dynamic behaviour is driven by the interaction between it's physical parameters (masses, dampings and stiffnesses), which is effectively revealed by the global sensitivity analysis applied here. In one sense the application of SA methods allows an evaluation of the robustness-to-uncertainty of the model as it establishes what the expected impact of variability on the model parameters would be on the model predictions. It could be argued that such an analysis would be more usefully used as a precursor to a calibration study as it would allow those parameters and interactions to which the predictions are most sensitive to be identified. However, this would be contingent upon feasible ranges for the parameters having already been specified. In this study those ranges arose from the system identification step.

Ultimately the study serves as a necessary step towards developing validation methods for nonlinear systems using the introduced experimental testbed. The next stage for the work is to complete the specification of the validation exercise for the structure in its linear state, then explicitly address the complications that arise once nonlinearity is introduced. Completing the validation exercise will involve specifying a criteria for accepting the model as 'valid', then evaluating the model performance against this criteria for a series of more demanding validation experiments, for example under structural modification. For the nonlinear system, there is additional interest in investigating whether validating a model based upon its ability to accurately predict time domain responses is a sufficient basis for ascribing credibility to its ability to predict responses in the frequency domain.

References

1. AIAA (1998) Guide for the verification and validation of computational fluid dynamics simulations (G-077-1998). American Institute of Aeronautics and Astronautics
2. ASME (2006) V&V 10 Guide for verification and validation in computational solid mechanics. American Society of Mechanical Engineers
3. ASME (2009) V&V 20 Standard for verification and validation in computational fluid dynamics and heat transfer. American Society of Mechanical Engineers
4. Homma T, Saltelli AK (1996) Importance measures in global sensitivity analysis of model outputs. Reliab Eng Syst Saf 52:1–17
5. Kennedy MC Gem-SA Homepage. Available from: http://ctcd.group.shef.ac.uk/gem.html
6. Kennedy MC, O'Hagan A (2001) Bayesian calibration of computer models. J R Stat Soc Ser B 63:425–464
7. Kennedy MC, Anderson CW, Conti S, OHagan A (2006) Case studies in Gaussian process modelling of computer codes. Reliab Eng Syst Saf 91:1301–1309
8. Matlab v7 (2004) The Mathworks
9. Oakley JE, O'Hagan A (2004) Probabilistic sensitivity analysis of complex models: a Bayesian approach. J R Stat Soc Ser B 66:751–769
10. Press WH, Teukolsky SA, Vetterling WT, Flannery BP (2007) Numerical recipes: the art of scientific computing, 3rd edn. Cambridge University Press
11. Price K, Storn R (1997) Differential evolution—a simple and efficient heuristic for global optimization over continuous spaces. J Glob Optim 11:341–359
12. Qin AK, Suganthan PN (2005) Self-adaptive differential evolution algorithm for numerical optimization. In: Proceedings of IEEE congress on evolutionary computation (CEC 2005), Edinburgh, Scotland
13. Sacks J, Welch WJ, Mitchell TJ, Wynn HP (1989) Design and analysis of computer experiments. Stat Sci 4:409–435
14. Saltelli AK, Chan A, Scott EM (2000) Sensitivity analysis. Wiley, New York
15. Worden K, Becker WE (2012) On the identification of hysteretic systems, part II: Bayesian sensitivity analysis and parameter confidence. Mech Syst Signal Process 29:213–227
16. Worden K, Manson G (2012) On the identification of hysteretic systems, part I: fitness landscapes and evolutionary identification. Mech Syst Signal Process 29:201–212